JMB

Available online at www.sciencedirect.com

ScienceDirect

ELSEVIER

COMMUNICATION

Crystal Structure of the First Plant Urease from Jack Bean: 83 Years of Journey from Its First Crystal to Molecular Structure†

Anuradha Balasubramanian and Karthe Ponnuraj*

Centre of Advanced Study in Crystallography and Biophysics, University of Madras, Guindy Campus, Chennai 600 025, India

Urease, a nickel-dependent metalloenzyme, is synthesized by plants, some bacteria, and fungi. It catalyzes the hydrolysis of urea into ammonia and carbon dioxide. Although the amino acid sequences of plant and bacterial ureases are closely related, some biological activities differ significantly. Plant ureases but not bacterial ureases possess insecticidal properties independent of its ureolytic activity. To date, the structural information is available only for bacterial ureases although the jack bean urease (*Canavalia ensiformis*; JBU), the best-studied plant urease, was the first enzyme to be crystallized in 1926. To better understand the biological properties of plant ureases including the mechanism of insecticidal activity, we initiated the structural studies on some of them. Here, we report the crystal structure of JBU, the first plant urease structure, at 2.05 Å resolution. The active-site architecture of JBU is similar to that of bacterial ureases containing a bi-nickel center. JBU has a bound phosphate and covalently modified residue (Cys592) by β-mercaptoethanol at its active site, and the concomitant binding of multiple inhibitors (phosphate and β-mercaptoethanol) is not observed so far in bacterial ureases. By correlating the structural information of JBU with the available biophysical and biochemical data on insecticidal properties of plant ureases, we hypothesize that the amphipathic β-hairpin located in the entomotoxic peptide region of plant ureases might form a membrane insertion β-barrel as found in β-pore-forming toxins.

© 2010 Elsevier Ltd. All rights reserved.

Keywords: jack bean urease; crystal structure; insecticidal properties; plant urease

Edited by M. Guss

Jack bean urease (*Canavalia ensiformis*; JBU) was the first enzyme to be crystallized, a feat accomplished by James. B. Sumner in 1926,[1] for which he was awarded Nobel Prize in chemistry in 1946. Sumner's work is very important in two aspects. First, it provided the proof about the proteinaceous nature of enzymes, and secondly, it demonstrated that proteins can be crystallized. Although JBU was the first enzyme to be crystallized, its structure is yet to be determined. JBU was also the first enzyme shown to contain nickel at its active site.[2]

Like urease, its substrate urea is also of major historical significance since it was the first organic compound to be synthesized in 1828.[3] Urea is a major nitrogenous waste product of biological actions. In general, urea is short-lived and rapidly metabolized by microbial activities. Urease (urea amidohydrolase EC 3.3.1.5) catalyzes the hydrolysis of urea to form ammonia and carbamate. The later compound spontaneously hydrolyzes at physiological pH to form carbonic acid and a second molecule of ammonia.[4]

Urease is produced by bacteria, fungi, yeast, and plants where it catalyzes the urea degradation to supply these organisms with a source of nitrogen for growth.[5] Ureolytic activity of bacteria such as *Clostridium perfringens*, *Klebsiella pneumoniae*, *Proteus*

---

† This work is dedicated in memory of Professor James B. Sumner.

Corresponding author. E-mail address: pkarthe@hotmail.com.

Abbreviations used: JBU, jack bean urease; BME, β-mercaptoethanol; DAP, diamidophosphoric acid; PFT, pore-forming toxin.

mirabilis, *Salmonella* sp., *Staphylococcus saprophyticus*, *Ureaplasma urealyticum*, and *Yersinia enterocolitica* plays an important role in the pathogenesis of human and animal diseases.[6,7] One of the most frequently studied bacterial urease is that from *Helicobacter pylori* since it has been implicated in peptic ulcers and stomach cancer.[8] In plants, urease is widely distributed in leguminous seeds and is suggested to play an important role in seed germination.[9] Plant ureases are also suggested to participate in seed chemical defense.[10]

Ureases are among the few enzymes that require nickel for activity. It is known that binding of nickel to urease is very specific and tight and the removal of metal ions can be achieved only by harsh treatment with denaturants or acids,[11–13] which is not the case in most other metalloenzymes. *In vivo* incorporation of nickel in both bacterial and plant ureases requires a set of accessory proteins that appear to act as urease-specific chaperones.[14]

Plant and fungal ureases are homo-oligomeric proteins of 90-kDa identical subunits, while bacterial ureases are multimers of two- or three-subunit complexes. The bacterial and plant ureases have high sequence similarity, suggesting that they have similar three-dimensional structures and a conserved catalytic mechanism.[6,15] Both bacterial and plant ureases display several biological activities that are independent of their ureolytic activity.[16–20] For example, enzymatic activity is not involved in platelet aggregation and antifungal activities of plant and microbial ureases.[17,19,20] Similarly, the lethal activity of canatoxin (an isoform of JBU) in mice and the insecticidal activity of plant ureases are independent of ureolytic activity.[16,17] It is interesting to note that, in spite of their closely related amino acid sequences, the insecticidal activity of ureases differ significantly among plant and bacterial ureases.[17] The insecticidal properties of plant ureases were first described for canatoxin[21] and later for JBU[17,22] and soybean seed-specific urease.[17]

To date, X-ray crystal structures of the native enzyme, mutants, and inhibitor complexes from three microbes, *Klebsiella aerogenes*, *Bacillus pasteurii*, and *H. pylori*, have been determined and analyzed.[23] Among the plant ureases, only the crystallization and preliminary X-ray analysis of JBU were reported earlier.[24,25] To better understand the biological properties of plant ureases, we initiated the structural studies on some of them and crystallized two ureases from pigeon pea and jack bean.[26,27]

Follmer[15,22] reported that the great heterogeneity, insolubility, and high polydispersity of JBU[5,28,29] in solution were the possible reasons for the failures in its structure determination by X-ray crystallography. We were successful in overcoming these shortcomings and have determined the structure of JBU, 83 years after its first crystals were obtained. In this article, we report the high-resolution structure of JBU, the first plant urease structure, and its comparison with the bacterial counterparts and the structural basis for the insecticidal property of plant ureases.

Structure of JBU monomer

Plant ureases are made up of single-chain polypeptide in contrast to bacterial ureases, which consist of two or three polypeptides designated as α, β, and γ (Fig. 1a).[6,15] Nevertheless, the bacterial ureases turned out to be homologous to plant ureases. The amino acid sequence alignment of JBU and bacterial ureases is shown in Fig. 1b and Fig. S1. JBU (840 residues, 90 kDa) has been crystallized in a hexagonal space group, $P6_322$, with one molecule in the asymmetric unit. JBU forms a hammer or T-shaped molecule, which is similar to its crystallographically characterized bacterial counterparts from *K. aerogenes* (KAU), *B. pasteurii* (BPU), and *H. pylori* (HPU).[30–32]
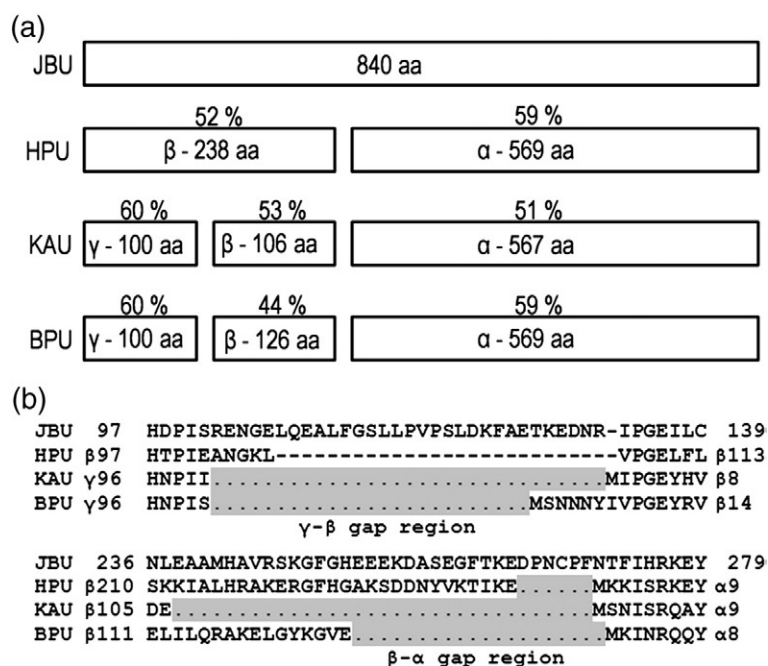

Fig. 1. Comparison of JBU and bacterial ureases. (a) Schematic comparison of a single structural subunit of JBU with two (*H. pylori*, HPU) and three [*K. aerogenes* (KAU), *B. pasteurii* (BPU)] subunits of bacterial ureases. With reference to JBU, the percentage identity of sequence of corresponding regions of bacterial ureases is indicated above the box. (b) Partial sequence alignment of JBU with HPU, KAU, and BPU. The highlighted region indicates the gap between γ–β and β–α domains of bacterial ureases.

The single-chain JBU monomer consists of four domains—the N-terminal αβ domain (1–134) forms the handle of the hammer, which is connected to another αβ domain (135–285) that forms one end of the hammer head. The second αβ domain is connected to a β domain (286–401 and 702–761), the middle region of the hammer head. This region is followed by a C-terminal (αβ)$_8$ TIM barrel domain (402–701 and 762–840), which is the other end of the hammer head and contains the active site. The structure of JBU monomer is shown in Fig. 2a. Structural comparison of JBU monomer with KAU, BPU, and HPU revealed that the position of the secondary structural elements remains conserved and their main chains superimpose with an rmsd of 0.60, 0.70, and 0.76 Å, respectively (Fig. 2b).

The major structural difference observed between JBU and bacterial ureases are at the gap regions between the γ, β, and α subunits (Fig. 1a and b) and

at a loop region that covers the active site. The first difference is at the region between β and α subunits, which is truncated in both two- and three-chained ureases. The sequence comparison of JBU with KAU, BPU, and HPU revealed that the gap region in between β and α subunits of bacterial ureases varies in length (Fig. 1b). In terms of number of residues, the length of the β–α gap in KAU and BPU are 33 and 20, respectively. In HPU, it is only 6 residues. In JBU, this insertion (β–α link) corresponds to amino acids Glu238-Phe270, which consist of an α-helix (233–246) and a long random-coil structure (247–270).

The second difference is at the gap between γ and β subunits, which is present only in three-chained ureases (KAU and BPU). In JBU, this region corresponds to amino acids Arg102-Arg132, which consist of a short loop (Arg102-Glu105), an α-helix (Leu106-Leu110), again a loop region (Leu111–Ser120), a 3$_{10}$ helix (Leu121-Lys123), followed by another loop
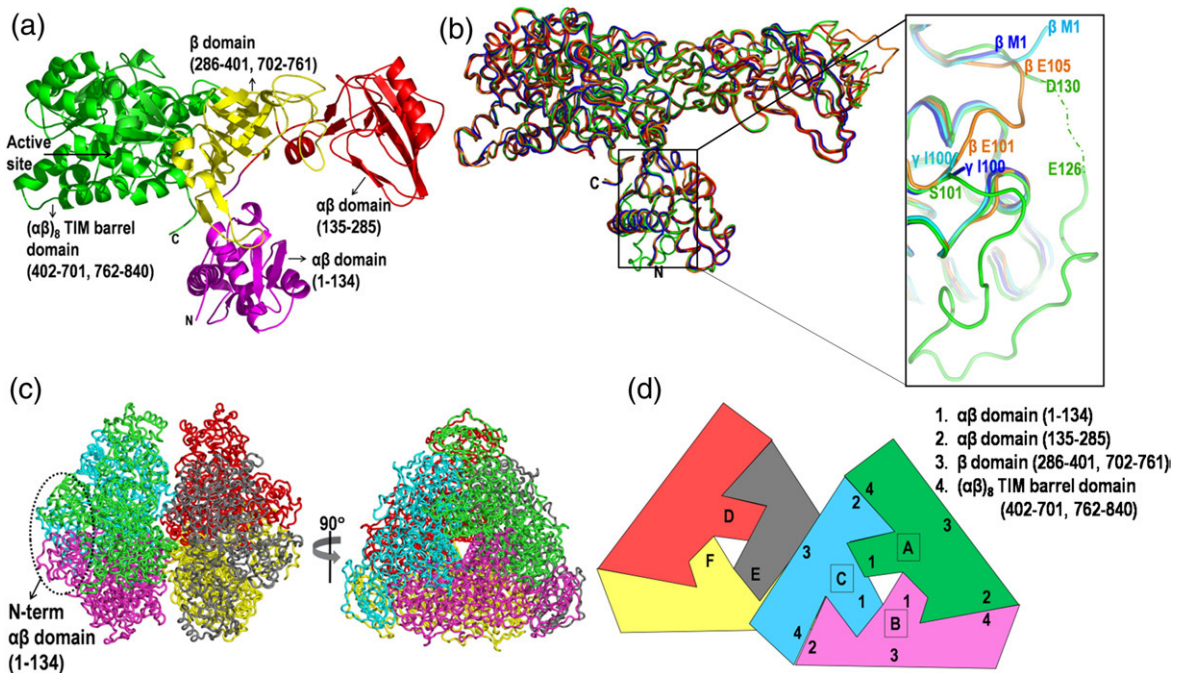

Fig. 2. Overall structure of JBU monomer, its oligomeric assembly, and comparison with its bacterial counterparts. (a) The isolation, purification, and crystallization of JBU have been described earlier.[27] In brief, JBU was purified from jack bean meal (Sigma) to a final concentration of 20 mg/mL and crystals were obtained by the hanging-drop vapor-diffusion method. A 2.05-Å native data set was collected at the XRD1 beamline of Elettra, Italy. Structure solution was achieved by molecular replacement using homology model of JBU derived from *H. pylori* urease (Protein Data Bank ID: 1E9Z). The final model was established after many cycles of manual rebuilding followed by refinement with an *R*-factor of 18.3% and an *R*$_{free}$ of 20.1%. Data collection and refinement statistics are given in Table S1. More details are given in the Supplementary Material. A hammer or T-shaped JBU monomer consists of four domains: the N-terminal αβ domain (magenta, handle of the hammer), another αβ domain (red, one end of the hammer head), a β domain (yellow, the middle region of the hammer head), and C-terminal (αβ)$_8$ TIM barrel domain (green, other end of the hammer head). (b) A backbone superposed structure of JBU (green) with native HPU (orange), native KAU (blue), and native BPU (cyan). The closer view shows the gap between γ and β domains of KAU and BPU. The corresponding region in JBU and HPU is linked by 31 and 5 residues, respectively. (c) The backbone representation of JBU hexamer. Three monomers are associated in a triangular fashion generating a planer surface on face of the triangle, whereas the other face has a small protrusion formed by the N-terminal αβ domain (1–134). The two trimers pack against one another through their planer surface and form a functional hexamer. View of the hexamer down the crystallographic 3-fold axis is shown in right. (d) Schematic representation of the hexamer. Molecules A, B, and C form a trimer with a head-to-tail packing of N-terminal αβ domain (135–285) of one molecule with the C-terminal (αβ)$_8$ TIM barrel domain (402–701 and 762–840) of another molecule in a cyclic nature.

region (Phe122-Arg132). Comparing two- and three-chained ureases in a two-chained urease (HPU), the single β subunit corresponds to γ and β subunits of a three-chained urease with a connection in between them. In both JBU and HPU, although the corresponding regions of the γ and β subunits of a three-chained urease is fused, in HPU a very short loop links these subunits in comparison to 31 residues looping out in JBU (Fig. 2b).

The third difference is observed in the helix–turn–helix motif (Met590-His607) that covers the active-site cavity. The conformation of this motif in JBU and its comparison with the corresponding region in KAU, BPU, and HPU are discussed in detail below.

Apart from these three major structural differences, there are also some small variations at many loop regions throughout JBU.

Oligomeric assembly

Previous reports suggest that JBU exists as a trimer or a hexamer of identical 90- kDa subunits,[2,11] with each subunit containing two nickel ions. Similar to JBU, bacterial ureases also form trimer or hexamer.[5] Based on gel-filtration chromatography and native gel electrophoretic analysis, JBU used for the present structural analysis was found to be a hexamer in solution. This is thus consistent with earlier biochemical characterization.

The crystallographic asymmetric unit contains one JBU molecule (molecule A) that packs against seven neighboring symmetry-related molecules (B, C, D, E, F, G, and H). Molecules A, B, C, D, E, and F generate the biologically active hexamer, a dimer of trimers (Fig. 2c and d), while molecules G and H are components of neighboring two-hexameric assembly. Molecules A, B, and C form one trimer whereas molecules D, E, and F form another trimer. In a trimer, the three monomers are associated very tightly in a triangular arrangement and disposed around the crystallographic 3-fold axis (Fig. 2c). Monomer A and its interaction with seven neighboring symmetry-related molecules involve 1667 inter-atomic interactions until 4.0 Å, of which 185 correspond to hydrogen bonds and 53.56% solvent-exposed area buried (Supplemental Table S2). In a trimer assembly, one face of the trimer has a small protrusion (Fig. 2c) formed by the N-terminal αβ domain ('handle' of the hammer) of the three monomers that interact with one another. The other face of the trimer is relatively planer and the two trimers pack against each other and interact through this planer surface via nine hydrogen bonds and 213 non-bonded interactions. Approximately 3040 Å² surface area of a trimer is buried at the trimer–trimer interface and this constitutes about 4.52% of the total surface area of each trimer. The trimer assembly in JBU is highly similar to the crystallographic trimers of KAU, BPU, and HPU as observed from the rmsd of 0.64, 2.59, and 0.78 Å, respectively, upon superposition of main-chain atoms. Like in KAU, BPU, and HPU, the formation of trimer in JBU is such that the N-terminal αβ domain (135–285) of molecule A

packs against the C-terminal $(\alpha\beta)_8$ TIM barrel domain (402–701 and 762–840) of molecule B and its αβ domain (135–285) packs against the C-terminal $(\alpha\beta)_8$ TIM barrel domain of molecule C in a cyclic head-to-tail fashion (Fig. 2d).

In previous mutagenesis experiments on KAU, it was shown that the conformation and stability of the molecule are remarkably insensitive to loss of nickel ions and active-site mutations.[33] Similarly, previous biochemical studies on JBU had shown that the enzyme exhibits remarkable resistance to denaturation by retaining 50% of its activity even after treatment with 2 M guanidinium chloride and 2.5 μM ethylenediaminetetraacetic acid at 38 °C for 2 h at pH 7.6, and 25% remains after treatment with 9 M urea, pH 9, at 25 °C for 24 h.[11] The structural analysis of JBU here revealed the presence of extensive intermolecular interactions in the hexameric assembly, which would provide the structure-based explanation for the abovementioned biochemical results since these interactions might be the key contributing factor for the enzyme's remarkable stability.

Active-site architecture

The sequence comparison of plant and bacterial ureases indicates that their catalytic sites display highly conserved amino acid residues (Fig. S1).[15] The catalytic site of JBU is very similar to that of bacterial ureases consisting of bi-nickel center with the nickel ions Ni1 and Ni2 separated by a distance of 3.7 Å. Residues His519 $N^{\delta 1}$, His545 $N^{\epsilon 1}$, and Lys490* $O^{\delta 1}$ are liganded to Ni1, while the residues His407 $N^{\epsilon 2}$, His409 $N^{\epsilon 2}$, Asp633 $O^{\delta 1}$, and Lys490* $O^{\delta 2}$ are liganded to Ni2. Lys490* is carbamylated and acts as a bridging residue between the two nickels. The superposition of active-site region of JBU with native KAU, BPU, and HPU revealed that the overall architecture is very similar (Fig. 3a). Hence, we here provide a limited description of the active site since the features of the bi-nickel center have been described previously in detail.[30,31]

During the refinement of the structure, the difference Fourier map unambiguously showed a tetrahedral-shaped density between the two nickel atoms, which was assumed to be four water/hydroxide molecules as found in native BPU and KAU. However, a positive peak was observed at the center of the tetrahedral density after assigning four water molecules. This indicated that the tetrahedral density could correspond to a phosphate group since it was already reported that the phosphate is a weak active-site inhibitor of urease.[11,34] In JBU crystallization, a high concentration of phosphate (1.6 M) was used as a precipitant; moreover, the position of the tetrahedral density in JBU exactly matches the position of the phosphate found in the phosphate-inhibited BPU structure.[35] Hence, the tetrahedral density in JBU was interpreted as phosphate and refinement was carried out. Phosphate moiety forms four coordination bonds with the two Ni ions. The phosphate oxygen atom $O^{\delta 4}$
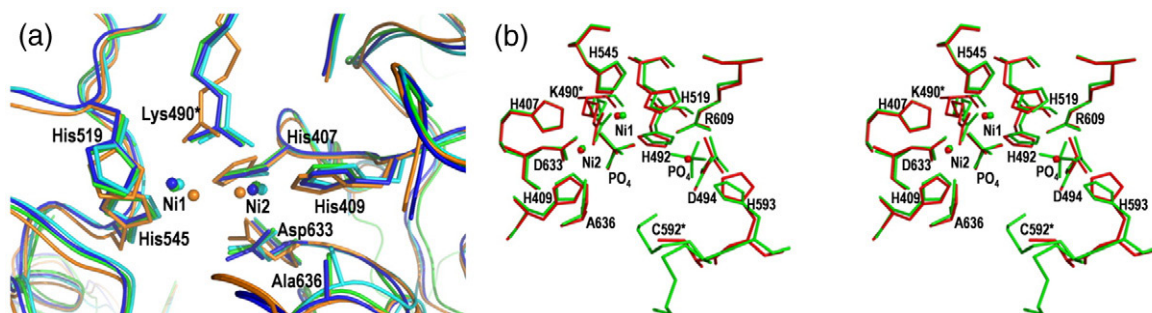
Fig. 3. Active site of JBU and bacterial ureases. (a) A superposition of the active site of JBU (green), native HPU (orange, 1E9Z), native KAU (blue, 1FWJ), and native BPU (cyan, 2UBP). The overall active-site architecture of JBU is very similar to that of bacterial ureases containing a bi-nickel center. (b) A stereo diagram of closer view of the superposition of active-site environment and Ni coordination of JBU (green) and phosphate–BPU (red, 1IE7). The active site of JBU contains two phosphates whereas in phosphate-inhibited BPU, a water molecule (red sphere) occupies the second phosphate position of JBU. The active-site residues in JBU/HPU/KAU/BPU are as follows: His407/136/134/137, His409/138/136/139, Lys490/219/217/220, His492/221/219/222, Asp494/223/221/224, His519/248/246/249, His545/274/272/275, Cys592/321/320/323, His593/322/320/323, Arg609/338/336/339, Asp633/362/360/363, and Ala636/365/363/366.

symmetrically bridges Ni1 and Ni2 at a distance of 2.12 and 2.20 Å, respectively, and thus replaces the bridging hydroxide molecule (W_B) present in the native KAU and BPU structures. The other two phosphate oxygen atoms such as $O^{\delta1}$ and $O^{\delta2}$ interact with Ni1 and Ni2 at a distance of 2.16 and 2.35 Å, respectively. The Ni1-bound phosphate oxygen forms an additional hydrogen bond with His^{492} ($N^{\varepsilon2}$) at 2.81 Å. The fourth phosphate oxygen $O^{\delta4}$ (distal) is directed into the active-site channel. Closer comparison of the active-site regions of JBU and phosphate-inhibited BPU indicates that the arrangements of protein ligands around the Ni ions in both the structures are essentially identical (Fig. 3b). Selected bond distances and angles around the bi-nickel center in JBU, KAU, and BPU are given in Supplemental Table S3.

It is interesting to note that in JBU, a disordered second tetrahedral density is found in close vicinity to the active site, which is not present in the phosphate-inhibited BPU structure. This density is also interpreted as phosphate, which makes 25 contacts with protein molecule with less than 4 Å including two hydrogen bonds: Arg609 (NH1) to P ($O^{\delta4}$) and Arg609 (NH2) to P($O^{\delta2}$) at a distance of 2.49 and 3.30 Å, respectively. The interesting aspect of this second phosphate is that its position in JBU exactly matches with the position of a sulfate in the native BPU structure,[31] where the sulfate interacts with Arg339 (equivalent to Arg609 of JBU) through hydrogen bond as observed in JBU.

A previous study shows that phosphate competitively inhibits KAU in the pH range of 5.0–7.0.[36] Similar results were obtained for JBU where the inhibition was found in the pH range of 5.8–7.5 using phosphate buffer at a concentration range of 0.53–123 mM.[37] In the present study, JBU was crystallized using ammonium phosphate as a precipitant in a Tris buffer of pH 8.8 (pH of the crystallization solution was found to be 8.2), which is significantly higher than the upper pH limit of the

phosphate buffer used in the inhibition studies. Despite this, phosphate was found at the active site of JBU probably because of its high concentration (1.6 M) in the crystallization solution. However, both the phosphates in the JBU structure exhibit only a partial occupancy as observed in the phosphate-inhibited BPU structure though the latter structure was crystallized at pH 6.3, which is well within the phosphate inhibition range.

In bacterial ureases, a mobile flap that covers the active site was suggested to play an important structural feature by exhibiting two different conformations through which the enzyme regulates both access of the substrate to the active site and the release of the reaction products.[30,38] The structural comparison of JBU with bacterial ureases revealed that the region Met590 to His607 of the TIM barrel domain form the mobile flap in JBU. In native KAU and HPU, this mobile flap adopts a 'closed' conformation, which is in contrast to the 'open' conformation found in the native BPU-inhibited, phosphate-inhibited,[35] β-mercaptoethanol (BME)-inhibited,[39] and acetohydroxamic acid-inhibited[40] BPU. However, the flap is 'closed' in diamidophosphoric acid (DAP)–BPU.[31] In JBU, the flap exhibits 'open' conformation (Fig. 4a). Site-directed mutagenesis and chemical modification experiments indicate that in bacterial ureases, this flap contains two key residues (His320 and Cys319 of KAU; His323 and Cys322 of BPU), which help in changing the flap conformation and in controlling the accessibility of the active site.[41] The 'closed' conformation of the flap seen in the DAP–BPU was changed to an 'open' conformation in the native BPU structure.[31] As a result of this 'closed' to 'open' flap movement, the residue His323 (His320 in KAU) located in the flap was displaced 5 Å (Fig. 4a), and in the 'open' flap structure, a sulfate molecule occupies where the imidazole ring of the His323 was previously positioned blocking the entry of
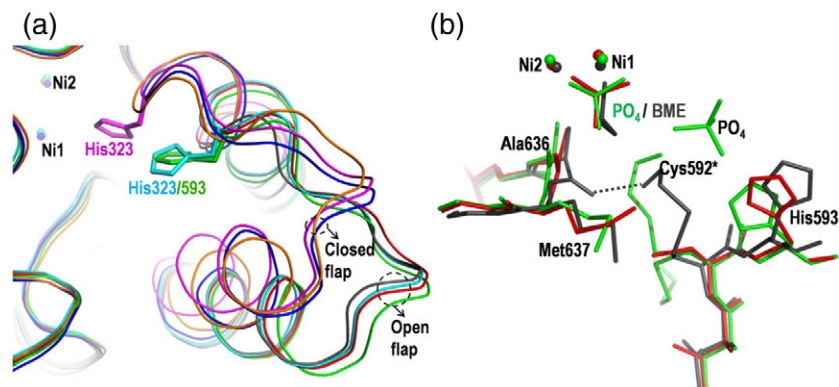
Fig. 4. Conformation of the active-site mobile flap and BME-modified Cys592* in JBU and bacterial ureases. (a) Overlay of residues Met590 to His607 of JBU (green), native KAU (blue, α317–334), native BPU (cyan, α320–337), native HPU (orange, α319–336), phosphate–BPU (red), BME–BPU (gray, 1UBP), and DAP–BPU (magenta, 3UBP). In JBU, native BPU, phosphate–BPU, and BME–BPU, the flap adopts similar conformation (open conformation), which is in contrast to the closed conformation seen in the native KAU, native HPU, and DAP–BPU structures. (b) Orientation of the carbonyl oxygen of Ala636 and BME-modified Cys592* in JBU (green). The corresponding residues in BME–BPU (gray) and phosphate–BPU (red) are also shown. In BME–BPU, the α-hydroxyl group of Cys322 forms a hydrogen bond with the carbonyl oxygen of Ala366 (gray dotted lines), which is not observed in JBU and phosphate–BPU. In JBU, Cys592* adopts double conformation ('*' indicates covalent modification of Cys592).

the active-site cleft. In the present JBU structure and in the phosphate-inhibited BPU, this sulfate is replaced by a phosphate (second phosphate) and a water molecule, respectively (Fig. 3b).

The other critical residue Cys319 (Cys322 in BPU, Cys592 in JBU) located on the mobile flap is highly conserved in many ureases (Fig. S1).[15] Moreover, Cys319 was found to be involved in many reactions that result in enzyme inhibition.[42] In JBU, it was demonstrated that chemical modification of all the cysteine residues impairs the activity.[43] In the present structure, three cysteines have undergone covalent modification by BME to Cys-S-S-CH2-CH2-OH. Although JBU contains 36 cysteines, only 3 of them (Cys59, Cys207, and Cys592) were modified by BME, which is present in the purification buffer at a concentration of 5 mM. In BME-inhibited BPU structure, two BME molecules were found, one at the active site coordinating with nickel ions and the second molecule was involved in a mixed disulfide bond with Cys322 as observed in JBU.[39] Comparison of the environment around Cys322 of BPU and its corresponding residue Cys592 of JBU revealed that in the former, the BME molecule attached to Cys322 is further involved in a hydrogen bond between its α-hydroxyl group and the carbonyl oxygen atom of Ala366, located on a neighboring loop. This interaction reduces the flexibility of the mobile flap and also restricts the accessibility of the active site. It is interesting to note that in JBU, although BME is involved in mixed disulfide bond with Cys592, its α-hydroxyl group does not form a hydrogen bond with carbonyl oxygen atom of Ala636 (equivalent of Ala366 of BPU) since the orientation of the carbonyl oxygen is different in comparison with its orientation in BPU (Fig. 4b). Furthermore, in JBU, the BME-modified Cys592 exhibits two different conformations, which is not observed in BPU.

In JBU, it was shown that the enzyme slowly loses its activity upon storage in the presence of BME and oxygen due to the formation of a mixed disulfide bond involving Cys592 and BME. In the same study, further it was demonstrated that the enzymatic activity can be restored by treatment of inactive urease with excess dithiothreitol, sulfite, or BME.[44] In the present structure, Cys592 is covalently modified by BME, which suggests that the enzyme is inactive. However, with excess dithiothreitol, sulfite, or BME, the reactivation of the enzyme is unlikely in the present structure since the active site contains one more inhibitor, which is phosphate.

Mechanism of urease activity

The mechanism of urease has been the subject of debate since the early 1920s.[45] From biochemical studies, crystal structures of native, site-directed variants, and inhibitor complexes of bacterial ureases of *K. aerogenes* and *B. pasteurii*, two mechanisms have been proposed.[30,31] In the enzymatic mechanism proposed based on the crystal structure of *K. aerogenes* enzyme, urea binds with its carbonyl oxygen bound to Ni1 and retaining a water molecule in the Ni2 site. Consequently, the active-site flap closes and the Ni2-bound hydroxide acts as a nucleophile and attacks the carbonyl carbon atom of the urea molecule, which is polarized by coordination to Ni1. The reaction proceeds through a tetrahedral intermediate that releases ammonia with His320 acting as a general acid.[41] In the other mechanism proposed by Benini *et al.*[31] for *B. pasteurii* enzyme, urea binds in a bidentate manner with its carbonyl oxygen bound to Ni1 and one of the amino group bound to Ni2, thus replacing three water moieties, leaving only the bridging hydroxide. This hydroxide attacks urea to give the tetrahedral transition state leading to formation of ammonia and

carbamate. However, the precise steps in catalysis remain unclear.

At the residue level, the active-site architecture of JBU matches very well with the corresponding region of phosphate-inhibited BPU (Fig. 3b), but the JBU active site is unique in a way that it has also features of native and BME-inhibited BPU. In the structure of phosphate–BPU complex, a water molecule positioned between distal oxygen of phosphate and Arg339 was suggested to play a role in catalysis.[35] This water molecule is not found in the JBU structure as observed in native BPU. In JBU, the water molecule is replaced by phosphate (second phosphate), and in native BPU, it was sulfate. However, in BME–BPU and acetohydroxamic acid–BPU, a similarly positioned water molecule was observed. In the BME–BPU structure, the residue Ala366 makes a hydrogen bond with α-hydroxyl group of BME molecule, which forms a mixed disulfide bond with Cys322. This hydrogen bond is not observed in either JBU or phosphate–BPU, although in JBU, Cys592 forms a mixed disulfide bond.

Proposed mechanism for insecticidal property

The plant ureases from soybean and jack bean (JBU and canatoxin) are shown to have insecticidal activity in insects with cathepsin B-based (cysteine protease) and cathepsin D-based (aspartyl protease) digestive system. In contrast, no effect was seen in insects relaying on trypsin-like digestive enzymes.[46,47] Interestingly, no change in the insecticidal effects of the jack bean and soybean ureases was observed after treatment of the enzymes with an irreversible inhibitor of ureolytic activity, indicating that insecticidal and ureolytic activities are unrelated.[17] It was shown that in canatoxin, its entomotoxic effect relies on an internal 10-kDa peptide (termed pepcanatox), released by hydrolysis of canatoxin by cathepsins in the digestive system of susceptible insects. Furthermore, a 13-kDa recombinant peptide called jaburetox-2Ec, analog to pepcanatox, was cloned in *E. coli* and was found to have insecticidal activity.[48] Contrasting with plant ureases, insecticidal activity was not seen in bacterial (*B. pasteurii*) urease[17] and it was postulated that the entomotoxic peptide released from canatoxin by insect cathepsins is absent in microbial ureases because the subunit structure is made up of two or three chains[17] and it is likely that the linker peptide that connects the different chains possess the insecticidal activity.

In fact, mapping the 10-kDa region, homologous to jaburetox-2Ec, in bacterial ureases corresponds to a region that includes the gap between the C-terminus of the β-chain and the N-terminus of the α-chain.[48] The sequence alignment of jaburetox-2Ec and its corresponding region in various plant and bacterial ureases is shown in Fig. 5a. This 10-kDa region in JBU structure (Gly230-Val320) consists of an α-helix, a long loop, another short helix, and a β-hairpin motif (Fig. 5b). A previous study of *ab initio* modeling of 10 kDa entomotoxic peptide predicts a β-hairpin motif within the peptide near its C-terminus and it was suggested that this motif may be responsible for the toxicity of jaburetox-2Ec by playing a role in either forming ion channel inhibition or pore formation.[48] This suggestion was made based on the observation that the β-hairpin motif of jaburetox-2Ec is structurally highly similar to ion channel inhibitors such as α-like neurotoxin BMK M1, β-neurotoxin, and BMKK4 and pore/channel-forming antimicrobial peptides such as protegrin-1, tachyplesin-1 and polyphemusin PV5.[49] The membrane-disruptive peptides can be grouped into three types: α-helix, β-sheet, and β-hairpin or loop.[50,51] The most prominent characteristic of these peptides is that they are largely amphipathic, with large portion of hydrophobic residues and positively charges residues.[52] This amphipathicity of the peptides allows them to partition into the membrane lipid bilayer.[53] The sequence comparison of various plant ureases revealed that the putative membrane-disruptive β-hairpin motif located in the 10-kDa entomotoxic peptide region is highly conserved and exhibits amphipathic character (Fig. 5a and b).

Pore-forming toxins (PFTs) are widely distributed membrane-damaging toxins and they insert either amphipathic α-helix or β-hairpin to produce well-defined pores in the plasma membrane of attacked cells.[54] A subgroup of PFTs known as β-PFTs is predicted to form β-barrels that insert into membranes to make pores. In β-PFTs the individual β-hairpin from one monomer pairs up with the neighboring β-hairpins of the other monomers and generates a β-barrel structure that spans the membrane.[55]

In a recent study, it has been shown that jaburetox-2Ec forms aggregates when exposed to pH 5.5, which is close to the pH conditions within the insect midgut where the peptide is formed and exerts its *in vivo* effects.[56] Furthermore, jaburetox-2Ec was recently proven to possess membrane-disruptive ability on acidic lipid bilayers and also form aggregates.[49]

At present, there is no evidence for the oligomerization of jaburetox-2Ec being necessary for expression for its entomotoxic effect. However, in the light of the abovementioned points, we hypothesize that the amphipathic β-hairpin located in the C-terminal region of 10 kDa entomotoxic peptide of plant ureases might form a membrane insertion β-barrel as found in β-PFTs. It is interesting to note that this β-hairpin motif and most of the N-terminal part of the β-hairpin motif are present in bacterial ureases also. However, in bacterial ureases, the β-hairpin motif is contributed by the α-chain and its N-terminal part is from the β-chain; hence, the 10-kDa region is not intact and is made up of two chains (Fig. 5a). Although the precise mechanism is not known, it is likely that the N-terminal part of the β-hairpin motif is required for the stability of the putative transmembrane β-barrel and since, in bacterial ureases, this region is not attached to the β-hairpin motif, the stability of the β-barrel may be compromised, which may be the reason for bacterial urease (*B. pasteurii*) not being lethal to insects.

JBU has been extensively studied in many applications in medical, agricultural, and industrial
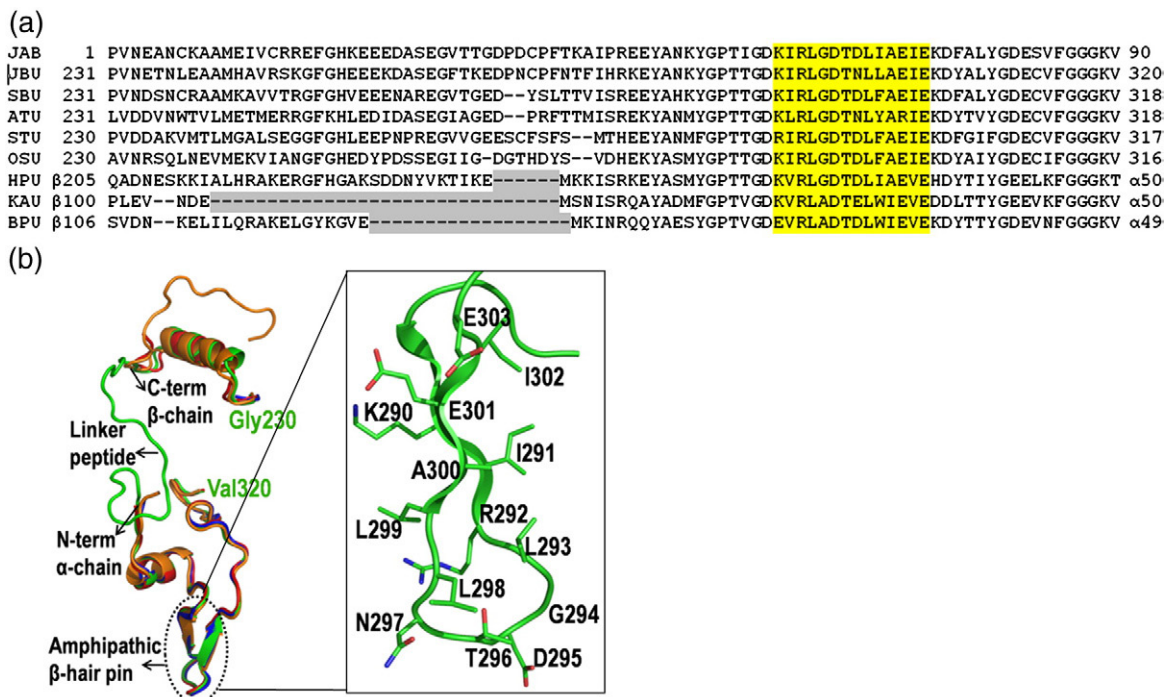
(a)

```
JAB   1 PVNEANCKAAMEIVCRREFGHKEEEDASEGVTTGDPDCPFTKAIPREEYANKYGPTIGDKIRLGDTDLIAEIEKDFALYGDESVFGGGKV  90
JBU 231 PVNETNLEAAMHAVRSKGFGHEEEKDASEGFTKEDPNCPFNTFIHRKEYANKYGPTTGDKIRLGDTNLLAEIEKDYALYGDECVFGGGKV 320
SBU 231 PVNDSNCRAAMKAVVTRGFGHVEEENAREGVTGED--YSLTTVISREEYAHKYGPTTGDKIRLGDTDLFAEIEKDFALYGDECVFGGGKV 318
ATU 231 LVDDVNWTVLMETMERRGFKHLEDIDASEGIAGED--PRFTTMISREKYANMYGPTTGDKLRLGDTNLYARIEKDYTVYGDECVFGGGKV 318
STU 230 PVDDAKVMTLMGALSEGGFGHLEEPNPREGVVGEESCFSFS--MTHEEYANMFGPTTGDRIRLGDTDLFAEIEKDFGIFGDECVFGGGKV 317
OSU 230 AVNRSQLNEVMEKVIANGFGHEDYPDSSEGIIG-DGTHDYS--VDHEKYASMYGPTTGDKIRLGDTDLFAEIEKDYAIYGDECIFGGGKV 316
HPU β205 QADNESKKIALHRAKERGFHGAKSDDNYVKTIKE------MKKISRKEYASMYGPTTGDKVRLGDTDLIAEVEHDYTIYGEELKFGGGKT α50
KAU β100 PLEV--NDE-----------------------------MSNISRQAYADMFGPTVGDKVRLADTELWIEVEDDLTTYGEEVKFGGGKV α50
BPU β106 SVDN--KELILQRAKELGYKGVE------------------MKINRQQYAESYGPTVGDEVRLADTDLWIEVEKDYTTYGDEVNFGGGKV α49
```

(b)

Fig. 5. Sequence comparison and the structure of the 10-kDa entomotoxic peptide region of JBU. (a) Sequence alignment of the 10-kDa entomotoxic peptide region of JBU and its corresponding region in various plant and bacterial ureases. The sequences are from Jaburetox-2Ec (JAB), *C. ensiformis* (JBU), *Glycine max* embryo-specific (SBU), *Arabidopsis thaliana* (ATU), *Solanum tuberosum* (STU), *Oryza sativa* (OSU), and bacterial ureases *H. pylori* (HPU), *K. aerogenes* (KAU), and *B. pasteurii* (BPU). The amphipathic β-hairpin region is indicated by yellow highlight. The gap between β and α chains of bacterial ureases is indicated by gray highlight. GenBank accession numbers of the sequences are given in the Supplementary Material. (b) Folding of the 10-kDa entomotoxic peptide region of JBU (Gly230-Val320, green) superposed with the corresponding region of native KAU (blue), native BPU (red), and native HPU (orange). In JBU, the insert corresponding to the gap between β and α chains of bacterial ureases is indicated as a linker peptide. The right panel shows residue-level detail of the amphipathic β-hairpin of JBU.

fields.[57] In agriculture, insect pests are a major cause of damage to the world's commercially important crops. Transgenic crops with intrinsic pest resistance offer a promising alternative for chemical pesticides to tackle the crop losses.[58] Since plant ureases exhibit insecticidal property, knowing their three-dimensional structure and the structural basis of the mode of action of its endomotoxic peptide could effectively be used for the development of insect-resistant transgenic plants. From the industrial point of view, a huge number of research papers have been published in the last four decades in JBU immobilization studies. JBU's structural integrity and significant resistance to chemical and thermal deactivation have been exploited extensively for immobilization studies. In this context, the present study reveals the quaternary structural details of JBU for the first time, which can be used by experimentalists and modelers to design better carriers for enzyme immobilization.

Protein Data Bank accession numbers

The atomic coordinates and structure factors have been deposited in the Protein Data Bank under accession number 3LA4.

References

1. Sumner, J. B. (1926). Isolation and crystallization of the enzyme urease. *J. Biol. Chem.* **69**, 435–441.
2. Dixon, N. E., Gazzola, C., Blakeley, R. L. & Zerner, B. (1975). Jack bean urease (EC 3.5.1.5). A metalloenzyme. A simple biological role for nickel? *J. Am. Chem. Soc.* **97**, 4131–4133.

3. Wöhler, F. (1828). Ueber künstliche Bildung des Harnstoffs. *Ann. Phys. Chem.* **12**, 253–256.

4. Andrews, R. K., Blakeley, R. L. & Zerner, B. (1984). Urea and urease. *Adv. Inorg. Biochem.* **6**, 245–283.

5. Mobley, H. L. T. & Hausinger, R. P. (1989). Microbial ureases: significance, regulation and molecular characterization. *Microbiol. Rev.* **53**, 85–103.

6. Mobley, H. L. T., Island, M. D. & Hausinger, R. P. (1995). Molecular biology of microbial ureases. *Microbiol. Rev.* **59**, 451–480.

7. Burne, R. A. & Chen, Y. M. (2000). Bacterial ureases in infectious diseases. *Microbes Infect.* **2**, 533–542.

8. Covacci, A., Telford, J. L., Del Giudice, G., Parsonnet, J. & Rappuoli, R. (1999). *Helicobacter pylori* virulence and genetic geography. *Science*, **284**, 1328–1333.

9. Zonia, L. E., Stebbins, N. E. & Polacco, J. C. (1995). Essential role of urease in germination of nitrogen-limited *Arabidopsis thaliana* seeds. *Plant Physiol.* **107**, 1097–1103.

10. Polacco, J. C. & Holland, M. A. (1993). Roles of urease in plant cells. *Int. Rev. Cytol.* **145**, 65–103.

11. Dixon, N. E., Riddles, P. W., Gazzola, C., Blakeley, R. L. & Zerner, B. (1980). Jack been urease (EC 3.5.1.5). II. The relationship between nickel, enzymatic activity, and the "abnormal" ultraviolet spectrum. The nickel content of jack beans. *Can. J. Biochem.* **58**, 474–480.

12. Zerner, B. (1991). Recent advances in the chemistry of an old enzyme: urease. *Bioorg. Chem.* **19**, 116–131.

13. Martin, P. R. & Hausinger, R. P. (1992). Site-directed mutagenesis of the active site cysteine in *Klebsiella aerogenes* urease. *J. Biol. Chem.* **267**, 20024–20027.

14. Moncrief, M. C. & Hausinger, R. P. (1996). Nickel incorporation into urease. In *Mechanisms of Metallocenter Assembly* (Hausinger, R. P., Eichhorn, G. L. & Marzilli, L. G., eds), pp. 151–171, Elsevier Press, New York, NY.

15. Follmer, C. (2008). Insights into the role and structure of plant ureases. *Phytochemistry*, **69**, 18–28.

16. Follmer, C., Barcellos, G. B., Zingali, R. B., Machado, O. L., Alves, E. W., Barja-Fidalgo, C. *et al.* (2001). Canatoxin, a toxic protein from jack beans (*Canavalia ensiformis*), is a variant form of urease (EC 3.5.1.5): biological effects of urease independent of its ureolytic activity. *Biochem. J.* **360**, 217–224.

17. Follmer, C., Real-Guerra, R., Wassermann, G. E., Olivera-Severo, D. & Carlini, C. R. (2004). Jackbean, soybean and *Bacillus pasteurii* ureases—biological effects unrelated to ureolytic activity. *Eur. J. Biochem.* **271**, 1357–1363.

18. Olivera-Severo, D., Wassermann, G. E. & Carlini, C. R. (2006). Ureases display biological effects independent of enzymatic activity: is there a connection to diseases caused by urease-producing bacteria? *Braz. J. Med. Biol. Res.* **39**, 851–861.

19. Olivera-Severo, D., Wassermann, G. E. & Carlini, C. R. (2006). *Bacillus pasteurii* urease shares with plant ureases the ability to induce aggregation of blood platelets. *Arch. Biochem. Biophys.* **452**, 149–155.

20. Becker-Ritt, A. B., Martinelli, A. H. S., Mitidieri, S., Feder, V., Wassermann, G. E., Santi, L. *et al.* (2007). Antifungal activity of plant and bacterial ureases. *Toxicon*, **50**, 971–983.

21. Carlini, C. R., Oliveira, A. E., Azambuja, P., Xaviera-Filho, J. & Wells, M. A. (1997). Biological effects of canatoxin in different insect models: evidence for a proteolytic activation of the toxin by insect cathepsin-like enzymes. *J. Econ. Entomol.* **90**, 340–348.

22. Follmer, C., Wassermann, G. E. & Carlini, C. R. (2004). Separation of jack bean (*Canavalia ensiformis*) urease isoforms by immobilized metal affinity chromatography and characterization of insecticidal properties unrelated to ureolytic activity. *Plant Sci.* **167**, 241–246.

23. Ciurli, S., Benini, S., Rypniewski, W. R., Wilson, K. S., Miletti, S. & Mangani, S. (1999). Structural properties of the nickel ions in urease: novel insights into the catalytic and inhibition mechanisms. *Coord. Chem. Rev.* **190–192**, 331–355.

24. Jabri, E., Lee, M. H., Hausinger, R. P. & Karplus, P. A. (1992). Preliminary crystallographic studies of urease from jack bean and from *Klebsiella aerogenes*. *J. Mol. Biol.* **227**, 934–937.

25. Sheridan, L., Wilmot, C. M., Cromie, K. D., Logt, P. V. D. & Phillips, S. E. V. (2002). Crystallization and preliminary X-ray structure determination of jack bean urease with a bound antibody fragment. *Acta Crystallogr., Sect. D: Biol. Crystallogr.* **58**, 374–376.

26. Balasubramanian, A. & Ponnuraj, K. (2008). Purification, crystallization and preliminary X-ray analysis of urease from pigeon pea (*Cajanus cajan*). *Acta Crystallogr., Sect. F*, **64**, 662–664.

27. Balasubramanian, A. & Ponnuraj, K. (2009). Purification, crystallization and preliminary X-ray analysis of urease from jack bean (*Canavalia ensiformis*). *Acta Crystallogr., Sect. F*, **65**, 949–951.

28. Fishbein, W. N., Spears, C. L. & Scurzi, W. (1969). Spectrum of urease isoenzymes: genetic, polymeric and conformeric. *Nature*, **223**, 191–193.

29. Fishbein, W. N. & Nagarajan, K. (1971). Urease catalysis and structure. VII. Factors involved in urease polymerization and its kinetic pattern. *Arch. Biochem. Biophys.* **144**, 709–714.

30. Jabri, E., Carr, M. B., Hausinger, R. P. & Karplus, P. A. (1995). The crystal structure of urease from *Klebsiella aerogenes*. *Science*, **268**, 998–1004.

31. Benini, S., Rypneiwski, W. R., Wilson, K. S., Meletti, S., Ciurli, S. & Mangani, S. (1999). A new proposal for urease mechanism based on the crystal structures of the native and inhibited enzyme from *Bacillus pasteurii*: why urea hydrolysis costs two nickels. *Structure*, **7**, 205–216.

32. Ha, N.-C., Oh, S.-T., Sung, J. Y., Cha, K. A., Lee, M. H. & Oh, B.-H. (2001). Supramolecular assembly and acid resistance of *Helicobacter pylori* urease. *Nat. Struct. Biol.* **8**, 505–509.

33. Park, I. S. & Hausinger, R. P. (1993). Site-directed mutagenesis of *Klebsiella aerogenes* urease: identification of histidine residues that appear to function in nickel ligation, substrate binding, and catalysis. *Protein Sci.* **2**, 1034–1041.

34. Howell, S. F. & Sumner, J. B. (1934). The specific effects of buffers upon urease activity. *J. Biol. Chem.* **104**, 619–626.

35. Benini, S., Rypneiwski, W. R., Wilson, K. S., Ciurli, S. & Mangani, S. (2001). Structure-based rationalization of urease inhibition by phosphate: novel insights into the enzyme mechanism. *J. Biol. Inorg. Chem.* **6**, 778–790.

36. Todd, M. J. & Hausinger, R. P. (1989). Competitive inhibitors of *Klebsiella aerogenes* urease. Mechanisms of interaction with the nickel active site. *J. Biol. Chem.* **264**, 15835–15842.

37. Krajewska, B. & Zaborska, W. (1999). The effect of phosphate buffer in the range of pH 5.80–8.07 on jack bean urease activity. *J. Mol. Catal. B: Enzym.* **6**, 75–81.

38. Moncrief, M. B. C., Hom, L. G., Jabri, E., Karplus, P. A. & Hausinger, R. P. (1995). Urease activity in the crystalline state. *Protein Sci.* **4**, 2234–2236.
39. Benini, S., Rypniewski, W. R., Wilson, K. S., Ciurli, S. & Mangani, S. (1998). The complex of *Bacillus pasteurii* urease with β-mercaptoethanol from X-ray data at 1.65-Å resolution. *J. Biol. Inorg. Chem.* **3**, 268–273.
40. Benini, S., Rypniewski, W. R., Wilson, K. S., Miletti, S., Ciurli, S. & Mangani, S. (2000). The complex of *Bacillus pasteurii* urease with acetohydroxamate anion from X-ray data at 1.55 Å resolution. *J. Biol. Inorg. Chem.* **5**, 110–118.
41. Karplus, P. A., Pearson, M. A. & Hausinger, R. P. (1997). 70 years of crystalline urease: what have we learnt? *Acc. Chem. Res.* **30**, 330–337.
42. Pearson, M. A., Michel, L. O., Hausinger, R. P. & Karplus, P. A. (1997). Structures of Cys319 variants and acetohydroxamate-inhibited *Klebsiella aerogenes* urease. *Biochemistry*, **38**, 8164–8172.
43. Juszkiewicz, A., Zaborska, A., Apta, A. & Olech, Z. (2004). A study on inhibition of Jack bean urease by garlic extract. *Food Chem.* **85**, 553–558.
44. Riddles, P. W., Andrews, R. K., Blakeley, R. L. & Zerner, B. (1983). Jack Bean urease VI. Determination of thiol and disulphide content. Reversible inactivation of enzyme by blocking of the unique cysteine residue. *Biochim. Biophys. Acta*, **743**, 115–120.
45. Mack, E. & Villars, D. E. (1923). Synthesis of urea with the enzyme urease. Action of urease in the decomposition of urea. *J. Am. Chem. Soc.* **45**, 505–510.
46. Ferreira-Dasilva, C. T., Gombarovits, M. E., Masuda, H., Oliveira, C. M. & Carlini, C. R. (2000). Proteolytic activation of canatoxin, a plant toxic protein, by insect cathepsin-like enzymes. *Arch. Insect Biochem. Physiol.* **44**, 162–171.
47. Carlini, C. R. & Grossi-de-Sa, M. F. (2002). Plant toxic proteins with insecticidal properties. A review on their potentialities as bioinsecticides. *Toxicon*, **40**, 1515–1539.
48. Mulinari, F., Staniscuaski, F., Bertholdo-Vargas, L. R., Postal, M., Oliveira-Neto, O. B., Rigden, D. J. *et al.* (2007). Jaburetox-2Ec: an insecticidal peptide derived

from an isoform of urease from the plant *Canavalia ensiformis*. *Peptides*, **28**, 2042–2050.
49. Barros, P. R., Stassen, H., Freitas, M. S., Carlini, C. R., Nascimento, M. A. C. & Follmer, C. (2009). Membrane-disruptive properties of the bioinsecticide Jaburetox-2Ec: implications to the mechanism of the action of insecticidal peptides derived from ureases. *Biochim. Biophys. Acta*, **1794**, 1848–1854.
50. Brogden, K. A. (2005). Antimicrobial peptides: pore formers or metabolic inhibitors in bacteria? *Nat. Rev. Microbiol.* **3**, 238–250.
51. Reddy, K., Yedery, R. & Aranha, C. (2004). Antimicrobial peptides: premises and promises. *Int. J. Antimicrob. Agents*, **24**, 536–547.
52. Hancock, R. E. W. (1997). Peptides antibiotics. *Lancet*, **349**, 418–422.
53. Hancock, R. E. W. & Rozek, A. (2002). Role of membranes in the activities of antimicrobial cationic peptides. *FEMS Microbiol. Lett.* **206**, 143–149.
54. Prevost, G., Menestrina, G., Colin, D. A., Werner, S., Bronner, S., Serra, M. D. *et al.* (2003). Staphylococcal bicomponent leucotoxins, mechanism of action, impact on cells and contribution to virulence. In *Pore-Forming Peptides and Protein Toxins* (Menestrina, G., Serra, M. D. & Lazarovici, P., eds), pp. 3–26, Taylor and Francis, London, UK.
55. Parker, M. W. (2003). Cryptic clues as to how water-soluble protein toxins form pores in membranes. *Toxicon*, **42**, 1–6.
56. Moro, C. F. (2007). Influence of chemical variables on the aggregation of the peptide insecticide derived from the urease from Jack bean (*Canavalia ensiformis*) for spectroscopy of light scattering. Porto Alegre: UFRGS, Conclusion Course (BS Chemistry), Institute Chemistry, Federal University of Rio Grande do Sul.
57. Qin, Y. & Cabral, J. M. S. (2002). Properties and applications of urease. *Biocatal. Biotransform.* **20**, 1–14.
58. Mohan Babu, R., Sajeena, A., Seetharaman, K. & Reddy, M. S. (2003). Advances in genetically engineered (transgenic) plants in pest management—an overview. *Crop Prot.* **22**, 1071–1086.